Optics and Lasers in Engineering 149 (2022) 106816

Contents lists available at ScienceDirect

Optics and Lasers in Engineering

journal homepage: www.elsevier.com/locate/optlaseng

Precise calibration of dynamic geometric parameters cameras for aerial mapping

Hongwen Zhang, Guoqin Yuan*, Xueji Liu

Key Laboratory of Airborne Optical Imaging and Measurement, Fine Mechanics and Physics, Chinese Academy of Science, Changchun Institute of Optics, Changchun 130033, China

ARTICLE INFO

Keywords:
Aerial mapping camera
Motion compensation
Geometric calibration
Distortion correction

ABSTRACT

Calibration is crucial for mapping cameras. Traditional calibration methods assume the geometric parameters are unchanged during the imaging process. However, aerial mapping cameras perform earth observation during a moving process. Owing to the forward flying of airplane, the exterior orientation parameters are changed during the exposure process. This leads to problems if directly applying the traditional methods to aerial mapping cameras. This paper presents a set of working time sequence and a new high-precision calibration method for aerial mapping cameras. We prove that the aerial mapping on a moving platform can be transformed into a mapping on a stationary platform by using the proposed method. Specifically, three steps are given to perform as follows. First, a proper distance is selected to decide a spot for the detector. We fix the detector at the selected spot and calibrate intrinsic parameters by exploiting traditional calibration methods. Second, the working time sequence of camera imaging is designed. The camera starts to expose an image and the exterior orientation parameters are obtained when the detector is driven to move to the calibrated spot. Third, a distortion model is proposed to correct distortions. We show that the dynamic measurement is identical to static measurement by using the proposed method. Experiments based on both simulated and real data are provided to show the effectiveness of the method.

1. Introduction

Aerial mapping cameras perform earth observation during a moving process and it is not possible to reduce the airspeed under a certain limits, which means there is a fast movement between the camera and the object. Therefore, Aerial mapping cameras need to consider the influence of motion on image quality. Otherwise, it will lead to the decline of mapping accuracy [1]. Film aerial cameras have been widely used in the early days. Due to their large frame, film cameras can use collimation mark and internal orientation technology, and perform forward motion compensation (FMC) to improve image quality and mapping precision. However, nowadays, film cameras are gradually being replaced by the digital camera due to the need of film chemically processed. Generally, traditional aerial digital mapping cameras cannot perform FMC because of CCD-matrix is not as large as film frame. However, FMC is a must to achieve high resolution images and mapping precise from low altitudes for medium to large scale applications [2]. Specifically, a camera system without FMC is limited to applications with medium to small photo-scale and can only be applicable for a low flight speed and a short exposure time [3]. To achieve a blur-free image and high mapping accuracy under large-scale mapping conditions, FMC is an absolute necessity for traditional digital mapping [4]. Aerial mapping camera with forward motion compensation (AMCWFMC) was one of the most important milestones in aerial photography of the last years [5]. For instance, the GTSZ camera developed by CIOMP drives the imaging detector to move reversely relative to the lens and compensates the motion between the camera and the object to achieve a high-quality imaging. Another is DMC camera, which has been successfully used all over the world and offers an outstanding ground resolution due to the fact that FMC is realized in time delayed integration (TDI) method [6].AMCWFMC is different from the traditional mapping camera and has prominent advantages including high-efficiency and high-precision mapping. AMCWFMC can provide high-precision products such as digital elevation model (DEM), digital orthophoto map (DOM) and digital line graph (DLG) [7–9].

Camera calibration is a necessary step to extract metric information from image when the acquired images are meant for metrology purposes [10]. With respect to the traditional cameras, many calibration methods have been developed [11–19]. Nevertheless, there are few reports about the calibration of AMCWFMC. Note that the interior and exterior orientation parameters are unchanged during the imaging process for traditional mapping cameras. However, these parameters are no longer unchanged for AMCWFMA owing to forward flying of airplane

* Corresponding author.
E-mail addresses: yuanguoqin@ciomp.ac.cn (G. Yuan), yuanguoqin@139.com (X. Liu).

https://doi.org/10.1016/j.optlaseng.2021.106816
Received 8 January 2021; Received in revised form 16 July 2021; Accepted 15 September 2021
Available online 8 October 2021

and the FMC. Furthermore, the distortion type is not known a prior. Thus, accurate calibration of AMCWFMC is still a challenging problem. However, the calibration technique for traditional camera is mature and can provide direct guide for the effectiveness of calibration method.

Classical calibration methods for cameras recover the projection mapping of the imaging system by the pinhole model [20] with supplemental polynomial corrections. One of the commonly used approaches is non-linear minimizing based on linear model [21,22] to estimate the calibration parameters including the interior and exterior orientation parameters and distortion polynomial coefficients. The parameters in pinhole model are assumed to be unchanged during the imaging process by traditional methods. Hence, there are several disadvantages by directly applying the traditional calibration methods to AMCWFMC. First, the exterior orientation parameters differ during the exposure time because of airplane motion. Second, the intrinsic parameters are changed as well due to the compensation motion of detector relative to lens. Third, the existing lens distortion mode is failed to calibrate the distortion of cameras when the detector moves. In one word, the traditional calibration methods are inapplicable for aerial mapping cameras.

In this paper, we propose a precise calibration method for AMCWFMC based on the pinhole model of the traditional calibration methods. First, we analyze the changing rules of the interior and exterior orientation parameters while camera is imaging under motion. Second, we constructively prove that the measurement under motion can be equivalent to a static measurement. Third, we establish the distortion model and propose the corresponding calibration method for AMCWFMC. At last, the effectiveness of the proposed method is verified by experiments based on both simulated and real data.

The rest of the paper is organized as follows. Some preliminaries, proof of applicability and proposed calibration method are given in Section II. The proposed distortion model is described in Section III. Results from validating the method both in simulation and on real data are presented in Section IV. Finally, Section V presents the conclusions.

2. Theoretical proof of equivalent measurement

2.1. Preliminaries

In principle, exposure time of cameras is supposed to be long enough (typically vary from 1/50 to 1/300 s.) to acquire energy for imaging [23]. The traditional camera does not move relative to the object during the exposure time. Thus, the exterior orientation parameters are constants. However, there is a rapid movement between aerial mapping cameras and the object during the exposure process. This leads to two severe issues (issue 1 and issue 2). First, the images obtained become blurred. Second, the exterior orientation parameters are changed at any time. The alteration can be up to a few meters.

FMC can deal with the first issue. Two images before and after FMC are given in Fig. 1. It can be seen that the image degrades substantially without FMC, which has a great impact on the measurement precision. Generally, FMC can be divided into mechanical method and TDI

(a). without motion compensation. (b). with motion compensation.

Fig. 1. Comparison of image quality before and after motion compensation. (a). without motion compensation. (b). with motion compensation.

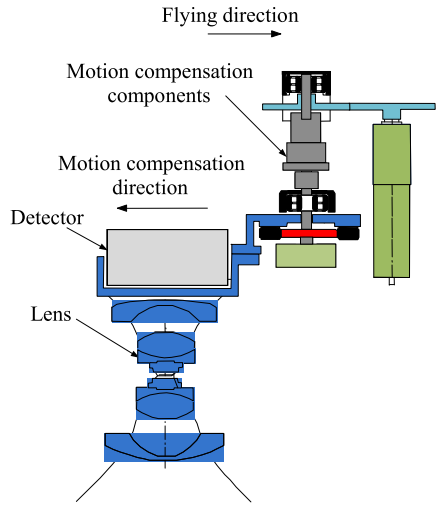

Fig. 2. Diagram of AMCWFMC in mechanical method.

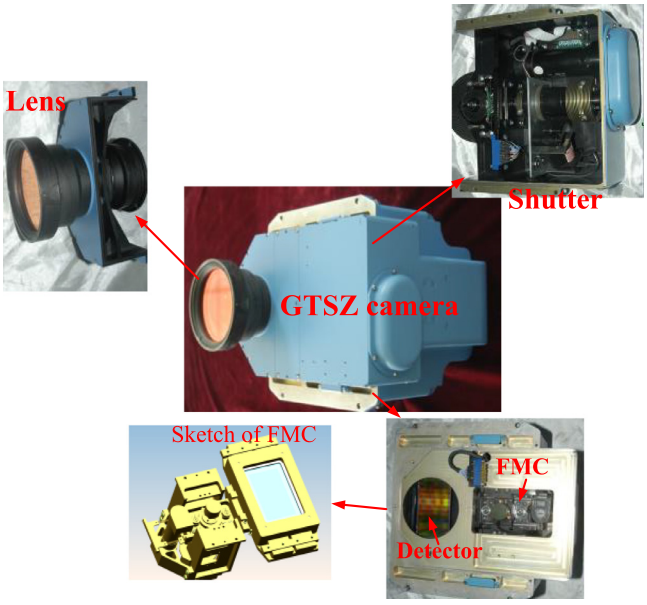

Fig. 3. General view of AMCWFMC (GTSZ camera).

method. In TDI method, FMC is accomplished by dividing the exposure time into a number of intervals, and composing a virtual frame by sampling the output of different physical pixels for each time interval, as the image moves across the focal plate. In mechanical method, the detector is driven by motion compensation components to reversely move relative to the lens as illustrated in Figs. 2 and 3. AMCWFMC consists of lens, detector, shutter and FMC components. The detector will be driven by FMC components to move relative to the lens to compensate for the relative motion between the camera and the object. The two methods have similar effects on calibration, so we take mechanical method as an example to introduce the proposed method, which is also applicable to TDI method.

According to optics, the principal point is exactly the perpendicular foot from the optical axis of lens to the detector [24–27]. Even though the relative motion of detector to lens solves the issue of image degradation, it causes another two issues (issue 3 and issue 4). First, the lens and the imaging sensor of the traditional aerial digital mapping cameras are integrated together and the lens distortion is unchanged. However AMCWFMC is not the case, to perform FMC, the imaging sensor will be driven to move relative to the lens, and the perpendicular foot from the

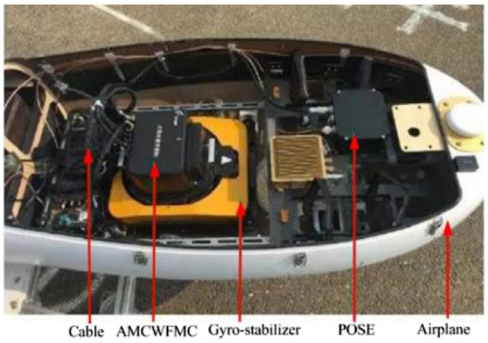

Fig. 4. Installation of camera and Gyro- stabilizer on the airplane.

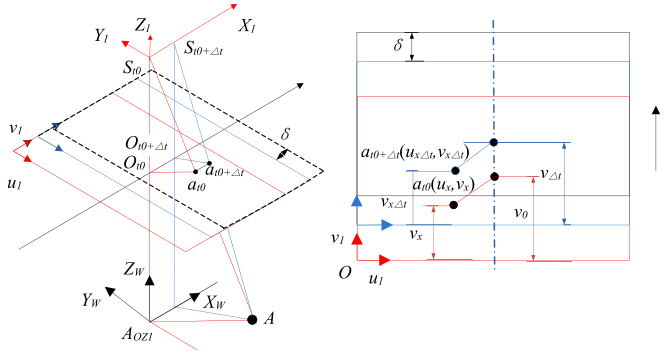

Fig. 5. Schematic diagram of central projection with FMC.

optical axis to the detector changes. Therefore, the principal point keeps changing as well (The change can be up to a few pixels). Second, the traditional distortion model is inapplicable for AMCWFMC.

2.2. Proof of applicability

In general, AMCWFMC is mounted on an airplane by a Gyro-stabilizer, which is shown in Fig. 4. A Gyro-stabilizer is a device that provides angular motion compensation, perfect vertical photography and automatic drift control for a wide range of airborne sensors. Hence, the Gyro-stabilizer can compensate for the variation of Euler angles during exposure process. Therefore, we only analyze the change of the position over exposure time.

For simplicity, at the beginning of imaging, i.e., t_0, the world coordinate system and image coordinate system are defined as follows. At time t_0, the intersection of optical axis of lens and the ground plane, i.e., A_{OZ1}, is chosen as the origin of the world coordinate system A_{OZ1}-$Z_W X_W Y_W$, as illustrated in Fig. 5. The flying direction and the optical axis of camera lens are chosen as X-axis and Z-axis, respectively. The pixel corner of the detector is chosen as the origin of the image coordinate system o-$u_1 v_1$, where v_1 is parallel to the X-axis of the world coordinate system. The image coordinate system is steadily connected to the detector, and move with the detector.

The exterior orientation parameters include the position and the orientation of a camera relative to the world coordinate system. Let$(X_{S_{t_0}}, Y_{S_{t_0}}, Z_{S_{t_0}})$denote the position of camera's exterior orientation parameters, (X_A, Y_A, Z_A)denote the coordinate of measured object in the world coordinate system, respectively. Let (u_0, v_0) and (u_x, v_x) be principal point $O_{t_0}$and the image of measured object A in the image coordinate system. At time $t_0 + \Delta t$ during the exposure process, the position of exterior orientation parameters is changed to $S_{t_0+\Delta t}(X_{t_0+\Delta t}, Y_{t_0+\Delta t}, Z_{t_0+\Delta t})$due to the forward motion of airplane. After FMC, the detector moves reversely with a displacement ofδ. Let$(u_{\Delta t}, v_{\Delta t})$, $(u_{x\Delta t}, v_{x\Delta t})$ be the coordinate of principal point $O_{t_0+\Delta t}$, the image of A in the image coordinate system, respectively.

Then, according to the pinhole model, at time t_0, we have [28].

$$\begin{aligned} \frac{X_A - X_{S_{t_0}}}{H} &= -\frac{u_x - u_0}{f} \\ \frac{Y_A - Y_{S_{t_0}}}{H} &= -\frac{v_x - v_0}{f}, \end{aligned} \tag{1}$$

Where f denotes principal distance of camera in pixels and $H = Z_{S_{t0}} - Z_A$represents the height of the airplane, respectively. Since the change of the X axis has a similar mathematical behavior as the Y axis, we only discuss the X axis here. For the position information of exterior orientation parameters at time t_0 and $t_0 + \Delta t$, the following relationship holds:

At time$t_0 + \Delta t$, we obtain

$$\frac{X_A - X_{S_{t_0}+\Delta t}}{Z_A - Z_{S_{t_0}+\Delta t}} = -\frac{u_{x\Delta t} - u_{\Delta t}}{f} \tag{2}$$

For the position information of exterior orientation parameters at time t_0 and $t_0 + \Delta t$, the following relationship holds:

$$\begin{aligned} X_{S_{t_0}+\Delta t} &= X_{S_{t_0}} + V\Delta t \\ Z_{S_{t_0}+\Delta t} &= Z_{S_{t_0}} \\ u_{\Delta t} &= u_0 + V_f \Delta t \end{aligned} \tag{3}$$

Where V denotes the flying speed of the airplane. V_f denotes the speed of FMC.

During the imaging process, the image point of A in the o-$u_1 v_1$ coordinate system is supposed to be unchanged owing to FMC. i.e.,

$$\begin{aligned} u_{x\Delta t} &= u_x \\ v_{x\Delta t} &= v_x \end{aligned} \tag{4}$$

Substituting Eqs. (3) and (4) into Eq. (2), yields

$$\frac{V\Delta t}{H} = \frac{V_f \Delta t}{f} \tag{5}$$

Define$FIM_{ou} = \frac{V\Delta t}{H}$, $IOE_{in} = \frac{V_f \Delta t}{f}$. It can be seen from Eq. (5) that FIM_{ou} represents the change amount of exterior orientation parameters at time $t_0 + \Delta t$ caused by flying and IOE_{in} refers to the change amount of the principal point in the intrinsic parameters measure in pixels at that time due to FMC. Eq. (5) indicates that the change of exterior orientation parameters caused by the forward flying of the airplane cancels out the change of intrinsic parameters caused by the FMC at any time in the imaging process. Therefore, we draw conclusions in the following.

(1) During the imaging process of AMCWFMC, the interior and exterior orientation parameters keep changing all the time. However, they cancel out each other when imaging at any given time. Since it has nothing to do with time, dynamic measurement is transformed into static measurement.

(2) During the imaging process of AMCWFMC, the imaging point of the measured object is fixed at the detector due to FMC. Thus, some issues such as tailing and blurring, caused by camera motion, can be avoided such that the imaging quality is improved. On the contrary, without FMC, the imaging of one measured object produces several image points due to the variations of exterior orientation parameters. It further results in many issues for images such as tailing, distortion and low resolution. Especially when the flying speed is large or exposure time is long, the image quality deteriorates significantly and imaging precision is substantially decreased. Thus, FMC is of essential importance to improve image quality.

(3) The measurement under motion can be equivalent to a static measurement through the proposed working time sequence and the calibration method. Theoretically, our method is applicable for cameras used for dynamic measurement and is not limited by zoom lens, flying speed, flying height and exposure time. But when the speed-to-height ratio is too large or the exposure time is too long, the speed and displacement of FMC will increase, which may lead to manufacturing difficulties.

4 Form the derivation process, factors affecting the accuracy of the proposed method is as follows: Eq. (1) is established under perfect vertical photography, so the stability of proposed method is affected by the accuracy of Gyro-stabilizer. Eq. (5) illustrates that V_f should be equal to $f^V/_H$. The accuracy of the FMC motion compensation has effect on the proposed method.

2.3. THE proposed calibration method

According to the analysis above, the steps of the calibration method of AMCWFMC can be summarized as follows.

(S1): Move the imaging detector relative to optical system to a certain point $\Delta\delta$and fix it ($\Delta\delta$ should be no less than the distance that the detector moves when it speeds from zero to the velocity required for FMC. FMC is a mechanical mechanism and self-locking mechanism can be added to the transmission chain. In this paper, worm gear mechanism is used to fix the detector.). Then, calibrate the intrinsic parameters including principal point, principal distance and distortion coefficients at this point in laboratory by exploiting the traditional calibration method, i.e., Zhang's method [29]. The procedure can be summarized as follow: the camera images the precisely measured calibration grids at different angles and the calibration parameters are obtained by solving the nonlinear equations according to the coordinates of the calibration grids and the image points. Two technologies are used to eliminate the changes of calibration parameters may be caused by inconsistency between the laboratory and actual condition. On the one hand, the airtight and thermal control technology is adopted to ensure that the environment is consistent. On the other hand, the calibration parameters are optimized by using aerial triangulation.

(S2): Design the working time sequence of AMCWFMC. When the motion compensation components drive the detector to move to the point$\Delta\delta$, camera starts to expose an image. Meanwhile, we acquire the exterior orientation parameters. By performing the two operations, the interior and exterior orientation parameters are accurately acquired at the same time. Note that the dynamic measurement is transformed into static one. Therefore, the issues 2 and 3 in Section 2 are solved.

S3): Analyze the distortion model to solve the issue 4 in Section 2. The reason why it is needed to analyze is as follows. The principal point varies during all the imaging process of AMCWFMC. The distortion caused by the variation affects the position of the image point. Thus, the traditional distortion model is inapplicable.

The flowchart of the proposed is shown in Fig. 6. The sequence diagrams are shown in Fig. 7.

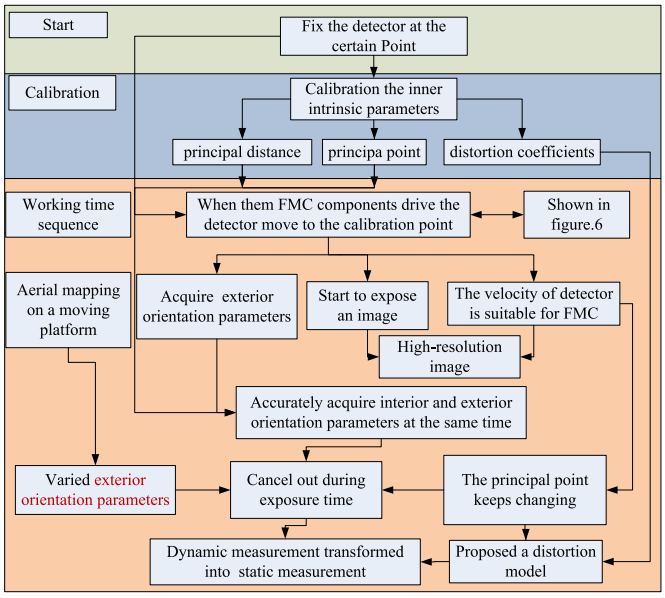

Fig. 6. Flowchart of the proposed method.

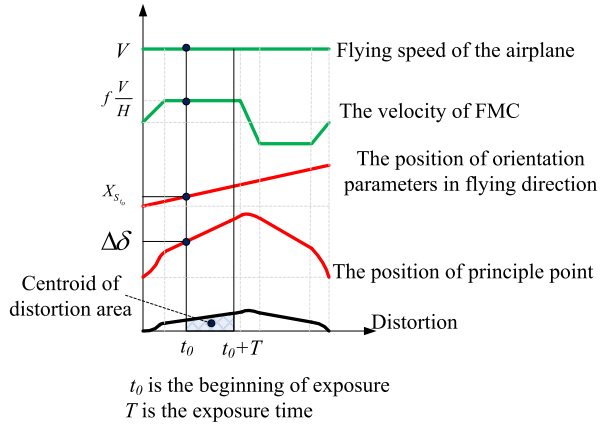

Fig. 7. Sequence diagrams of the proposed method.

3. The distortion model for AMCWFMC

3.1. THE impact factors for distortion

Distortion is an intrinsic defect for optical measuring system. The distortion is defined as the difference between the real and the theoretical image point after the object is imaging by imaging system.

According to optical aberration theory, Camera distortion can be divided into radial distortion, eccentric distortion, etc. Long-focus aerial mapping cameras generally require precise optical adjustment. The eccentricity of the optical lens is small, and the main distortion type is radial distortion. For most mapping camera, it is enough to consider only the first second order. Therefore, this paper only considers radial distortion. Considering too many kinds of distortions will lead to computational instability. The radial distortion $\Delta P_x, \Delta P_y$of image point (x, y) can be expressed as

$$\begin{aligned}\Delta P_x &= \phi(x_0, y_0) = K_1\bar{x}r^2 + K_2\bar{x}r^4\\ \Delta P_y &= \varphi(x_0, y_0) = K_1\bar{y}r^2 + K_2\bar{y}r^4.\end{aligned} \tag{6}$$

Where$\bar{x} = x - x_0, \bar{y} = y - y_0, r^2 = (x - x_0)^2 + (y - y_0)^2$ and (x_0, y_0) denotes the coordinate of the principal point.

According to Eq. (6), the distortion changes with the principle point. That is why the traditional distortion model is inapplicable here.

3.2. The variation of principle point and impact on distortion during fmc period

Note that the motion of the imaging detector relative to the lens leads to the variation of perpendicular foot of optical axis in the image plane. According to the definition of principal point, it varies during all the imaging process.

The main distortion type of AMCWFMC is radial distortion. According to the properties of the radial distortion [30], at time t_0 and$t_0 + \Delta t$, we obtain

$$A_{OZ1}A//a_{t_0}O_{t_o},\ A_{OZ2}A//a_{t_0+\Delta t}O_{t_0+\Delta t}$$

Where A_{OZ1} and A_{OZ2} denote the intersection of optical axis and the ground at time t_0 and$t_0 + \Delta t$, respectively. It can be rewritten as

$$\begin{cases}A_{OZ1}A \times a_{t_0}O_{t_o} = 0\\ A_{OZ2}A \times a_{t_0+\Delta t}O_{t_0+\Delta t} = 0\end{cases}$$

Then, we arrive at

$$\begin{cases}(v_x - v_{t_o})(X_A - X_{S_{t_o}}) - (u_x - u_{t_o})(Y_A - Y_{S_{t_o}}) = 0\\ (v_x - v_{t_o+\Delta t})(X_A - X_{t_o+\Delta t}) - (u_x - u_{t_o+\Delta t})(Y_A - Y_{t_o+\Delta t}) = 0\end{cases}$$

Table 1
Parameters for experiments of AMCWFMC.

Parameters	Values
Focal length	56.03mm
Pixel dimension	5μm
$\Delta\delta$	1000pixs
Distortion coefficients at $\Delta\delta$	K1 = 4.7249e-6, K2 = −2.2441e-9
Principal point at $\Delta\delta$	(45.674 mm,24.339 mm)
Typical height	1000 m
Typical velocity	230.4 km/h
Typical exposure time	1/100 s
The accuracy of the Gyro-stabilizer(Residual deviation form vertical photography)	0.1°
The displacement accuracy of FMC in typical exposure time	1/3 pixel

By solving the two equations, we have

$$v_{t_0+\Delta t} - v_{t_0} = f\frac{V}{H}\Delta t \tag{7}$$

When the period of exposure time is t, the overall variation of the principal point is

$$\delta = \int_0^t (v_{t_0+\Delta t} - v_{t_0})dt = \int_0^t f\frac{V}{H}dt = f\frac{V}{H}t \tag{8}$$

According to the properties of motion compensation components, the variation of the principal point is composed of two parts. The first part, produced before the beginning of exposure t_0, is the moving distance $\Delta\delta$of the detector driven by motion compensation components relative to optical system. During the moving period, the detector speeds up from zero to the velocity required for compensation. Since the intrinsic parameters are calibrated at $\Delta\delta$, this part has no impact on the measurement. The second part, produced from time $t_0$to the end of exposure, is the displacement of the detector δ. During the moving process, the camera is exposing an image while the principal point is changing. Thus, the distortion of image point keeps changing all the time. As a result, the distortion of the final image point becomes the centroid of distortion area during the exposure. It can be obtained by employing the first form curve integral [31]. Let $\Delta P'_{x2}$and $\Delta P'_{y2}$be the distortion caused by motion compensation. Then, we have

$$\begin{cases} \Delta P'_{x2} = \dfrac{\int_L x ds}{\int_L ds} = \dfrac{\int_0^\delta \phi(x_0,y_0)\sqrt{\phi'^2(x_0,y_0)+\varphi'^2(x_0,y_0)}dx_0}{\int_0^\delta \sqrt{\phi'^2(x_0,y_0)+\varphi'^2(x_0,y_0)}dx_0} \\ \Delta P'_{y2} = \dfrac{\int_L y ds}{\int_L ds} = \dfrac{\int_0^\delta \varphi(x_0,y_0)\sqrt{\phi'^2(x_0,y_0)+\varphi'^2(x_0,y_0)}dx_0}{\int_0^\delta \sqrt{\phi'^2(x_0,y_0)+\varphi'^2(x_0,y_0)}dx_0} \end{cases} \tag{9}$$

Eq. (9) presents the expression of the distortion resulted from motion compensation. It can be solved through the use of Simpson's rule.

4. Experiments and results

In this section, the proposed distortion model is verified by numerical simulation. Meanwhile, the proposed calibration method is verified by real data. The parameters used in the following experiments for AMCWFMC are given in Table 1.

4.1. Verification by numerical simulation

It can be seen from Table 1 that the variation of camera's exterior orientation parameters caused by flying is 0.64 m during exposure time. The image obtained is significantly blurred and distorted, as illustrated in Fig. 1. According to Eq. (8), the principal point moves 7.17 pixels caused by FMC during the exposure process. From Eq. (9), the distortion of image point varies over all the exposure time because of the position variation of the principal point. The relationship between the distortion of image point and the change of principal point for AMCWFMC is depicted in Fig. 8.

In Fig. 8, it can be seen that the distortion of image point changes with the variation of principal points. Note that both the value and the direction of the distortion are altered. The distortion during the exposure time for the top right-hand corner image point is plotted in Fig. 9. It can be seen that the change amount is more than one pixel.

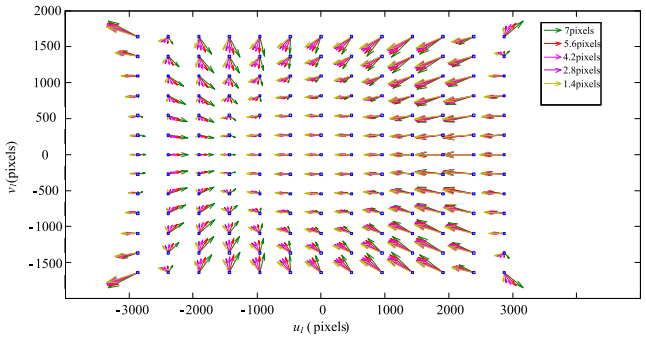

Fig. 8. The distortion of image point for different positions of principal point (1.4pixs, 2.8pixs, 4.2pixs, 5.6pixs and 7pixs).

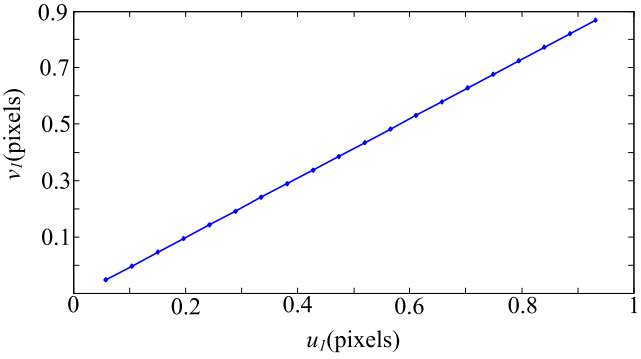

Fig. 9. The distortion of a certain image point during the exposure time.

Table 2
Comparison of the errors for the proposed distortion method and traditional distortion method.

	The proposed method	The traditional method
Maximal error (pixels)	0.05	3.7
RMSE (pixels)	0.018	1.45

In practice, grayscale extraction algorithm is a typical method to measure the coordinates of the image point [32,33]. Thus, the image point of the curve in Fig. 9 is measured by utilizing grayscale extraction algorithm. We compare the errors of the proposed distortion method with that of the tradition distortion method in Table 2. The proposed method corrects the distortion by using Eq. (9) after the exposure time. It can be clearly seen that the proposed method has much smaller errors than the traditional approach. Thus, the image precision is improved by using the proposed method.

Table 3
Summary of statistic results for residual errors using different calibration methods.

	Method 1	Method 2	Method 3
Number of check points	47	47	47
Maximum error in the aerial triangulation (pixel)	1.86	3.1	12.5
RMSE in the aerial triangulation (pixel)	0.76	1.75	4.8
Maximum error of plane in the orthophoto generation(m)	0.17	0.28	1.13
RMSE of plane in the orthophoto generation(m)	0.091	0.1228	0.45137
Maximum error of elevation in the orthophoto generation(m)	0.45	0.66	3.45
RMSE of plane elevation in the orthophoto generation(m)	0.387	0.659	1.897

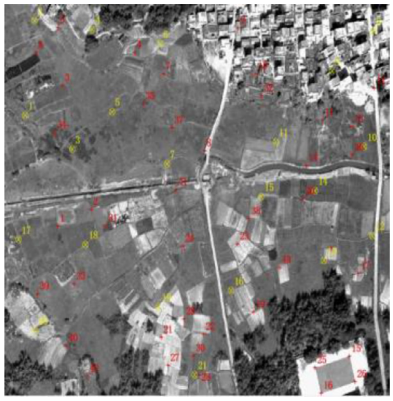

Fig. 10. The distribution of the 21 control points which are shown as yellow and the 43 check points which are shown as red in the area.

Fig. 11. Measure the control points and check points using RTK method.

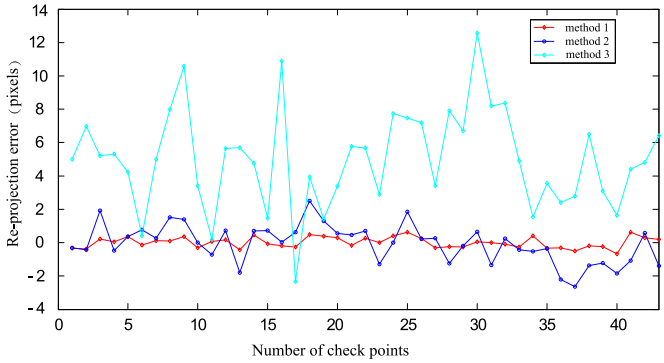

Fig. 12. *Re*-projection error for three different methods.

4.2. Flying experiments with real data

To verify the effectiveness of the proposed calibration method, experiments based on real data are performed. Firstly, we fix the imaging detector at the certain point and calibrate the intrinsic parameters. The results are set as shown in Table 1. Then, we chose an area of 10 km^2 and make a flight experiment. The parameters are set as shown in Table 1 including the flying height, flying speed, the accuracy of Gyro-stabilizer, and exposure time. There are 60 precision-measured points placed on the ground. These points are measured by Global Navigation Satellite System (GNSS) Real Time Kinematic (RTK) method. The measuring equipment is survey-grade GNSS receivers I70 made by CHC-NAV. The positions accuracy for points is centimeter-level. The measured points distributed in the clear signs such as roads, intersections and so on. Among the points, there are 21 control points and 43 check points. The details are shown in the Figs. 10 and 11.

The evaluation criterions are the re-projection error and the pixel value difference between the actual point and the calculated projection point. Taking the measured 3D points projected in the cameras with the camera calibration parameters again, obtaining new points in the camera. Then calculate the pixel value between the original points and the "re-projected" ones.

We use three different methods in the following to compute the re-projection error.

Method 1: The proposed calibration method and distortion model, with FMC.

Method 2: The proposed calibration method and the traditional distortion model, with FMC.

Method 3: the traditional calibration method and traditional distortion model, without FMC.

In the process of aerial image data processing, it mainly goes through two steps: aerial triangulation and orthophoto generation. We use three methods to calculate the re-projection error of aerial triangulation and orthophoto generation. The corresponding numerical statistical results are illustrated in Fig. 12 and Table 3. It can be seen that the method 3 has a significant systematic error and the re-projection error is the largest, which is due to the fact that there is no compensation for the variation of camera's exterior orientation elements caused by flying.

By comparing method 1 and method 2, it can be seen that the proposed distortion model promotes the maximum value of re-projection error from 3.1 pixels to 1.86 pixels compared with the traditional distortion method. The precision is improved by using the proposed method.

By comprehensive comparison of method 1 and method 3, it can be seen that FMC can significantly improve the measurement accuracy when there is relative motion between the camera and the object. We can see that the proposed method promotes the maximum value of re-projection error from 12.5 pixels to 1.86 pixels in the process of aerial triangulation. From the Table 3, we can see that the proposed method promotes RMSE of plane in the orthophoto generation from 0.45 m to 0.091 m, and promotes RMSE of elevation in the orthophoto generation from 1.897 to 0.387 m, which proves that the method 1 can effectively improve the mapping accuracy.

The following conclusions can be drawn through the experiment:

(1) When there is relative motion between the cameras and objects, such as in the flight of the aircraft, it will lead the exterior orientation parameters to be in a changing state. There will be problems if the traditional geometric calibration method (method (3) is still adopted.

(2) The proposed method is effective and the dynamic measurement can be transformed into static measurement.

(3) The experimental results show that in the experimental circumstances shown in Table 1, the proposed method effectively improves the mapping accuracy. It indicates that most Gyro-stabilizer can meet the requirements of the proposed method.

5. Conclusions

In this paper, we proved that the interior and exterior orientation parameters for cameras cancel out each other at any time of FMC process, so the interior and exterior orientation parameters at any time point can be used. We also derived the distortion model of cameras, and then a precise three-step calibration method for AMCWFMC was proposed. In the first step, select a proper to decide a point for the detector, move the detector at this point and fix it. Calibrate the elements of interior orientation by exploiting traditional calibration methods. In the second step, design the working time sequence of cameras. When the motion compensation components drive the detector to move to the point, the camera starts to expose an image. Meanwhile, the exterior orientation parameters are acquired. In the third step, correct the distortion according to the proposed distortion model. In this step, note that we conduct the transformation from the dynamic measurement to static measurement. The effectiveness and efficiency of the proposed calibration method and the distortion model were verified through numerical simulation and real data. Experiments demonstrate that the proposed method outperforms the traditional method. In particular, the proposed method promotes the maximum value of re-projection error from 12.5 pixels to 1.86 pixels compared with the traditional method without FMC in the process of aerial triangulation . The proposed method promotes RMSE of plane in the orthophoto generation from 0.45 to 0.091 m, and promotes RMSE of elevation in the orthophoto generation from 1.897 to 0.387 m.

In practice, however, there may be two problems. First, due to some unavoidable uncertainties in actual engineering, such as that of manufacturing and assembly errors, the displacement of the detector has bias. It implies that the interior and exterior orientation parameters do not cancel out accurately. Second, due to optical axis displacement relative to image plane, the image may become blur because of the distortion of image point varies over all the exposure time. Therefore, in future work, first, we will analyze the errors of the motion compensation components and expound the way to correct. Second, we will research on real-time distortion correction. Third, we will apply the proposed calibration method to several applications where have a fast movement between the camera and the object, such as industrial measurement (for example, the camera is fixed and the object being measured is place on a moving conveyor belt) and computer vision.

Declaration of Competing Interest

The authors declare that they have no known competing financial interests or personal relationships that could have appeared to influence the work reported in this paper.

CRediT authorship contribution statement

Hongwen Zhang: Conceptualization, Methodology, Supervision. **Guoqin Yuan:** Data curation, Writing – original draft. **Xueji Liu:** Validation, Writing – review & editing.

Acknowledgment

This work was supported in part by the National Science and Technology Major Project of China (No. 30-H32A01–9005–13 /15).

References

[1] Zhen R, Stevenson R. Multi-image motion deblurring aided by inertial sensors. J Electron Imaging 2016;25(1):013027.
[2] Ghosh SK. Image motion compensation through augmented collinearity equations. Proc SPIE Int Soc Opt Eng 1985;491:837–42.
[3] Zeth U. New features of the LMK aerial camera system. Jena Rev 1987.
[4] Heier H, Fritsch D, Spiller R. Deploying DMC in today's workflow. Proceedings of Photogrammetric Week Stuttgart 2001:35–45.
[5] Craig J. Comparison of Leica ADS40 and Z/I imaging DMC high-resolution airborne sensors. Proc SPIE Int Soc Opt Eng 2005;5655:270–80.
[6] Hinz A, Drstel C, Heier H. DMC - The Digital Sensor Technology of Z/I-Imaging. d.fritsch & r.spiller photogrammetric week 2003:93–103.
[7] Baltsavias E, Li Z, Eisenbeiss H. DSM Generation and interior orientation determination of IKONOS images using a testfield in Switzerland. Photogramm Fernerkund Geoinf 2009;2006.
[8] Sun B, Zhu J, Linghui Y, Yang S, Zhiyuan N. Calibration of line-scan cameras for precision measurement. Appl Opt 2016;55(25):6836–43.
[9] Lee M, Kim H, Paik J. Correction of barrel distortion in fisheye lens images using image-based estimation of distortion parameters. IEEE Access 2019;7:45723–33.
[10] Liu H, Linghui Y, Guo Y, Guan R, Zhu J. Precise calibration of linear camera equipped with cylindrical lenses using a radial basis function-based mapping technique. Opt Express 2015;23:3412.
[11] Lee M. Correction of barrel distortion in fisheye lens images using image-based estimation of distortion parameters. IEEE Access 2019;7:45723–32.
[12] Tsai R. A versatile camera calibration technique for high-accuracy 3d machine vision metrology using off-the-shelf TV cameras and lenses. IEEE J Robot Autom 1987;3:323–44.
[13] Schuster R, Braunecker B. The calibration of the ADC (Airborne digital camera) System, international archives of photogrammetry and remote sensing, 2000:288–294.
[14] Yuan G, Zheng L, Sun J, Liu X, Wang X, Zhang Z. Practical calibration method for aerial mapping camera based on multiple pinhole collimator. IEEE Access 2019;8(1):39725–33.
[15] Zheng L, Yuan G, Leng X, Wu Y. Calibration method for mapping camera based on a precise grouped approach method. Int J Pattern Recognit Artif Int 2018;32(11):20241–8.
[16] Bauer M, Grießbach D, Hermerschmidt A, Krüger S, Scheele M, Schischmanow A. Geometrical camera calibration with diffractive optical elements. Opt Express 2009;16:20241–8.
[17] Thibault S, Arfaoui A, Desaulniers P. Cross-diffractive optical elements for wide angle geometric camera calibration. Opt Lett Oct. 2011;36(24):4770–2.
[18] Gorevoy AV, Machikhin AS, Batshev VI, Kolyuchkin VY. Optimization of stereoscopic imager performance by computer simulation of geometrical calibration using optical design software. Opt Express 2019;27(13):17819–39.
[19] Genovese K, Chi Y, Pan B. Stereo-camera calibration for large-scale DIC measurements with active phase targets and planar mirrors. Opt Express 2019;27(6):9040–53.
[20] Toutin T. Review article: geometric processing of remote sensing images: models, algorithms and methods. Int J Remote Sens Int J Remote Sens 2004;25(10).
[21] Ricolfe-Viala C, Sanchez-Salmeron AJ. Camera calibration under optimal conditions. Opt Express 2011;19(11):10769–75.
[22] Ricolfe-Viala C, Sánchez-Salmerón AJ, Berti E. Accurate calibration with highly distorted images. Appl Opt 2012;51(1):89–101.
[23] Li X, Gao H, Yu C, Chen Z. Impact analysis of Lens shutter of aerial camera on image plane illuminance. Optik Jul. 2018;173 (Stuttg).
[24] Fischer RE. Optical system design. New York, NY, USA: McGraw-Hill; 2000.
[25] Lenz RK, Tsai RY. Techniques for Calibration of the Scale Factor and Image Center for High Accuracy 3-D Machine Vision Metrology. IEEE Transactions on Pattern Analysis and Machine Intelligence 1988;10(5):713–20.
[26] Willson RC, Shafer SA. What is the center of the image. IEEE Computer Society Conference on Computer Vision & Pattern Recognition 1994:2946–55.
[27] Fang Y, Zhang X, Li B, Sun N. A geometric method for calibration of the image center, The 2011 International Conference on Advanced Mechatronic Systems, 2011:6-10.
[28] Piteri S. Accuracy of mapping by panoramic photography. Earth Moon Planets Earth Moon Planet 1988;40:29–44.
[29] Zhang Z. A flexible new technique for camera calibration. IEEE Trans Pattern Anal Mach Intell 2000;22(11):1330–4.
[30] Wei GQ, Dema S. IMPLICIT AND EXPLICIT CAMERA CALIBRATION - THEORY AND EXPERIMENTS. IEEE Transactions on Pattern Analysis and Machine Intelligence 1994;16(5):469–80.
[31] Giordano FR, Hass J, Weir MD. Thomas' CALCULUS, alternate edition. UK: Addison Wesley Longman; 2002.
[32] Rufino G, Accardo D. Enhancement of the centroiding algorithm for star tracker measure refinement. Acta Astronaut Jul. 2003;53:135–47.
[33] Alexander BF, Kim CN. Elimination of systematic error in subpixel accuracy centroid estimation. Optical Engineering Jan. 1991;30(9):1320–30.